arXiv:1604.05137v1 [cond-mat.mtrl-sci] 18 Apr 2016

Itinerant G-type antiferromagnetism in $D0_3$-type V_3Z (Z=Al, Ga, In) compounds: A first-principles study

Iosif Galanakis[1],* Şaban Tırpancı[2], Kemal Özdoğan[3], and Ersoy Şaşıoğlu[4†]
[1]*Department of Materials Science, School of Natural Sciences, University of Patras, GR-26504 Patra, Greece*
[2]*Department of Physics, Gebze Technical University 41400 Gebze, Kocaeli, Turkey*
[3]*Department of Physics, Yildiz Technical University, 34210 İstanbul, Turkey*
[4]*Peter Grünberg Institut and Institute for Advanced Simulation, Forschungszentrum Jülich and JARA, D-52425 Jülich, Germany*
(Dated: April 19, 2016)

Heusler compounds are widely studied due to their variety of magnetic properties making them ideal candidates for spintronic and magnetoelectronic applications. V_3Al in its metastable $D0_3$-type Heusler structure is a prototype for a rare antiferromagnetic gapless behavior. We provide an extensive study on the electronic and magnetic properties of V_3Al, V_3Ga and V_3In compounds based on state-of-the-art electronic structure calculations. We show that the ground state for all three is a G-type itinerant antiferromagnetic gapless semiconductor. The large antiferromagnetic exchange interactions lead to very high Néel temperatures, which are predicted to be around 1000 K. The coexistence of the gapless and antiferromagnetic behaviors in these compounds can be explained considering the simultaneous presence of three V atoms at the unit cell using arguments which have been employed for usual inverse Heusler compounds. We expect that our study on these compounds to enhance further the interest on them towards the optimization of their growth conditions and their eventual incorporation in devices.

PACS numbers: 75.50.Pp, 75.47.Pq, , 75.30.-m

I. INTRODUCTION

The constant growth of computational materials science triggered an even more exciting growth in experimental materials science. Several phenomena have been explained based on ab-initio electronic structure calculations and several compounds with predefined properties targeting at specific applications have been studied. Among them exist the so-called half-metallic Heusler[1] compounds a special class of magnets which present semiconducting behavior for one of the two spin channels.[2,3] Several Heusler compounds have been identified using ab-initio calculations prior to their experimental growth.[4,5] Such materials can find a variety of applications in the field of magnetoelectronics (nanoelectronics where only magnetic materials are employed) and spintronics (nanoelectronics where hybrid devices of semiconductors and magnetic materials are used).[6] We should note here that there are also other known half-metals like $La_{0.7}Sr_{0.3}MnO_3$ which have been also demonstrated to present fully spin-polarized tunnelling in magnetic tunnel junctions,[7] but Heusler compounds remain very attractive for applications due to their very high Curie temperatures and their structural similarity to binary semiconductors.[8,9]

The most studied Heusler compounds in literature are the so-called full Heuslers having the chemical formula X_2YZ, like Co_2MnSi, and several have been identified as half-metals.[10] When the valence of the X is smaller than the valence of the Y they are called inverse Heusler compounds and crystallize in a similar structure where only the sequence of the atoms changes.[11] Also most of the latter compounds are half-metallic magnets.[11] Although the compounds referred to above can find several applications in spintronics and magnetoelectronics,[12] several half-metallic Heusler compounds with more exotic properties have been found which can further optimize the operation of devices. Among them are the so-called spin-gapless semiconducting (SGS)[13] Heuslers which present a usual semiconducting band structure for one spin direction and a gapless (almost or exactly zero energy gap) in the other spin-direction.[14,15] Such materials can enhance the performance of devices since vanishing energy is needed to excite both electrons and holes and a prototype Mn_2CoAl has been already grown experimentally and its SGS properties have been confirmed.[16]

A material of special interest is V_3Al, a Heusler compound crystallizing in the so-called $D0_3$ lattice structure shown in Fig. 1 which resembles the cubic structure of full-Heuslers where now all X an Y atoms are identical adopted also by other materials like Fe_3Al, Fe_3Si, and Cr_3Se.[17,18] The first attempt to study this material using first-principles calculations predicted a non-magnetic ground state.[19] But latter calculations by Skaftouros and collaborators predicted that the ground state is in reality an antiferromagnetic gapless semiconductor[14] resembling the well-known gapless semiconductors.[20] Such an electronic structure is possible since as shown in Fig. 1 there are two V atoms sitting at the A and C sites which form a simple cubic structure, if we neglect the other sites. The V atoms at these sites are allowed due to symmetry to have antiparallel spin magnetic moments of the same size leading to G-type antiferromagnetism shown schematically also in Fig. 1. The V atoms at the B sites and the Al atoms at the D sites are at the center of a cube surrounded by four V atoms at A sites

and four V atoms at C sites and thus due to symmetry reasons their spin magnetic moment in such a configuration should be zero. This is compatible with the so-called Slater-Pauling rule connecting the total number of valence electrons to the total spin magnetic moment in Heusler compounds.[11] In 2015 Jamer and collaborators presented an extensive study on V_3Al combining both electronic structure calculations and experiments.[21] On one hand their simulations confirmed the results of Skaftouros *et al*, and on the other hand they have successfully grown films of V_3Al and dichroic experiments using synchrotron radiation were compatible with an antiferromagnetic state. Here we have to note that the ground state of V_3Al is not the Heusler structure but the A15 lattice structure and V_3Al in this structure is a well-known superconductor.[22,23]

V_3Al can be viewed as a prototype material for studying gapless antiferromagnetic behavior and can be considered as a cornerstone for future spintronic and magnetoelectronic devices based on antiferromagnetic elements. Thus in present paper we provide an extensive study based on simulations of the electronic and magnetic properties of V_3Al as well as of the stability of its antiferromagnetic character. To make our study more complete we have also included results on V_3Ga and V_3In compounds which have the same number of valence electrons. Also these compounds were found to be antiferromagnetic gapless semiconductors and thus we will mainly concentrate on V_3Al but conclusions are also valid for them. In Sec. II we shortly present the computational method. In Sec. III A we discuss the electronic properties and the gapless behavior of the V_3Al compound under study and in Sec. III B its magnetic properties including also the calculation of the exchange constants and the Néel temperature. Sec. III C is devoted to the origin of the gapless behavior. Finally in Sec. IV we summarize and present our conclusions. We believe that our present results will even further intensify the interest on this unique compound.

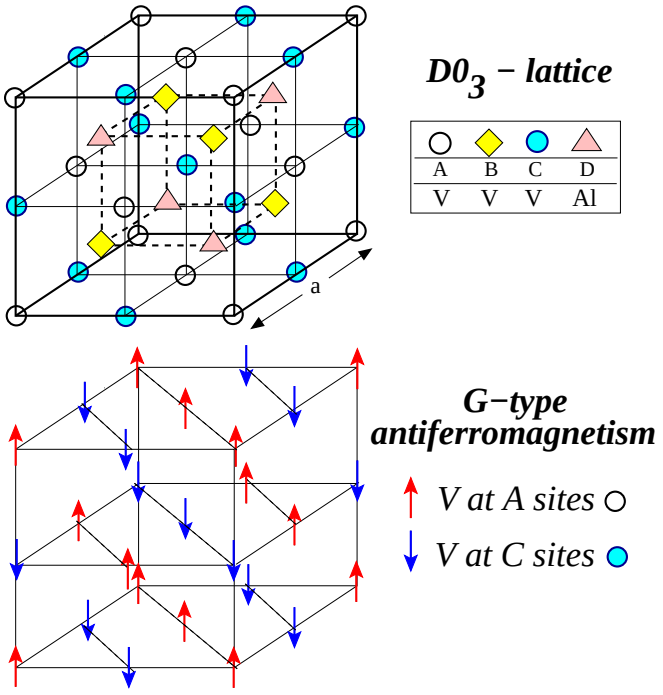

FIG. 1: (Color online) Upper panel: Schematic representation of the cubic $D0_3$ structure adopted by the V_3Z Heusler compounds. The unit cell is that of an f.c.c. with four equidistant atoms as basis along the [111] diagonal. The atoms at the A and C sites are at the center of a cube surrounded by four atoms at the B and four atoms at the C sites and vice versa. The V next-nearest neighboring atoms at the A and C sites for a lattice of octahedral symmetry if we neglect the B and D sites.
Lower panel: Schematic representation of the G-type antiferromagnetic order made up of successive (111) planes which are antiferromagnetically coupled. The V atoms at the A and C sites have antiparallel spin magnetic moments denoted by arrows of opposite direction. The V atoms at the B sites and the Al atoms have zero spin magnetic moments due to symmetry reasons being situated at the center of cubes having four V atoms at the A sites and four V atoms at C sites as nearest neighbors.

II. COMPUTATIONAL METHOD

To perform the electronic structure calculations, we employed the full-potential nonorthogonal local-orbital minimum-basis band structure scheme (FPLO)[24,25] within the generalized gradient approximation (GGA) as parameterized by Perdew, Burke and Ernzerhof.[26] Some of the results presented in Secs. III A and III B have been also obtained using the local-spin-density approximation (LSDA).[27] We have used the lattice parameter of 6.09 Å calculated via total energy calculations also using the FPLO method within GGA in Ref. 14. Using the same method we have also calculated the equilibrium lattice constants for the other two compounds and found a value of 6.07 Å and 6.32 Å for V_3Ga and V_3In, respectively (see Table I). For the integrations in the first Brillouin zone a dense Monkhorst-Pack grid has been used.[28] All results presented in this study have been obtained using FPLO with the exception of the exchange constants and Néel temperature in Sec. III B, which are obtained employing the ASW method.[29].

To calculate interatomic exchange parameters we employ the frozen-magnon technique[30–32] as described in Refs. 33 and 34. The Néel temperature is estimated by employing the so-called random-phase-approximation (RPA) approach.[34–38]

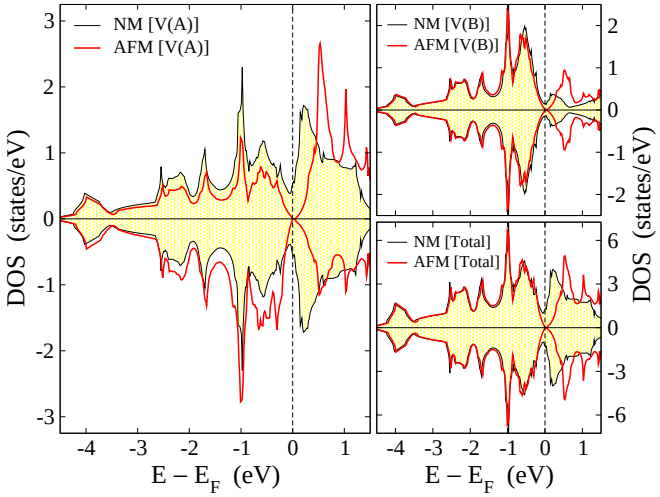

FIG. 2: (Color online) Total and atom-resolved density of states (DOS) within GGA for the non-magnetic (NM) and antiferromagnetic (AFM) magnetic configurations of V_3Al. Positive (Negative) DOS values corresponds to the spin-up (spin-down) electrons. The Fermi level corresponds to the zero energy.

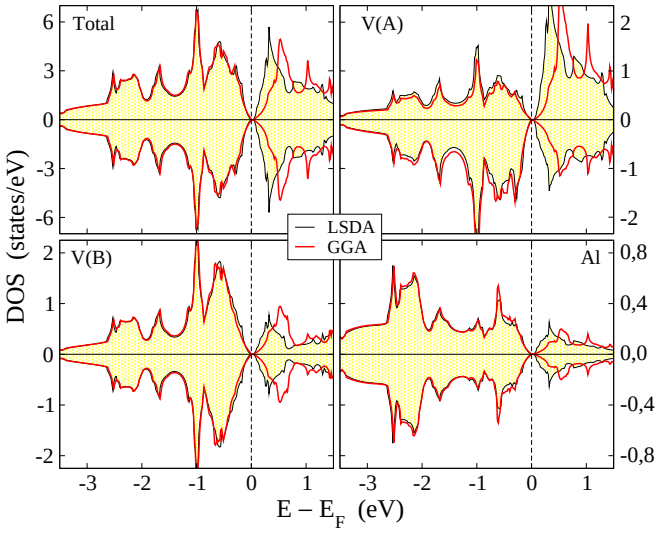

FIG. 3: (Color online) GGA vs LSDA calculated DOS for the antiferromagnetic V_2Al compound. Details as in Fig. 2.

III. RESULTS AND DISCUSSION

A. Electronic properties and gapless behavior

First, we should establish the gapless behavior of V_3Al. To this end in Fig. 2 we have plotted the density of states (DOS) projected on the V atoms at the A and B sites (the site is written either in parenthesis or as superscript to distinguish the V atoms) as well as the total one in the unit cell for both the non magnetic (NM) and the antiferromagnetic (AFM) configurations. We should first note that we cannot use the terms majority and minority spin since there is equal number of electrons of different spin in the formula unit; we will use the term spin-up for the positive DOS values and spin-down for the negative DOS values. We have also chosen the spin-up in the case of the V^A atoms such that its spin magnetic moment in Table I is negative. In the AFM case the DOS of the V^C atoms is identical to the V^A atoms exchanging the spin-up and spin-down electronic states. In the AFM case one gets a gapless behavior and the valence and conduction bands touch each other at the Fermi level. If we compare the NM and AFM calculations, most of the changes occur at the V^A DOS where the weight of the states around the Fermi level increases and we have a normal semiconductor. Deeper in energy the NM and AFM DOS are almost identical. Especially for the V^B atoms the DOS below the Fermi level is identical for both NM and AFM calculations. This also may explain the stability of the AFM case. A close examination of the total DOS reveals that the NM and AFM DOS are similar throughout most the energy range but at the Fermi level the zero DOS at the AFM case leads to smaller values of the total energy stabilizing it against the NM case where more electronic charge is present at the Fermi level.

To establish the gapless semiconductor we have also performed calculations using the LSDA functional and present them in Fig. 3 versus the GGA results. LSDA is well-known to underestimate the equilibrium lattice constants and to overestimate hybridization between orbitals with respect to GGA but for the same lattice constant both LSDA and GGA should produce similar electronic properties. This is true since also LSDA reproduces the gapless semiconducting behavior of GGA. The only noticeable difference between the two functional is the distribution of the weight of the unoccupied states just above the Fermi level. LSDA yields a smaller exchange splitting between d-states of different spin a the V^A and V^C states and thus there is a small shift of the unoccupied states towards smaller energy values which also reflects on the DOS of the V^B and Al atoms.

B. G-type antiferromagnetism: stability, magnetic moments, exchange constants and T_N

In this subsection we will discuss the magnetic properties of the compounds under study. In Table I we have included the energy difference ΔE between the non-magnetic and the antiferromagnetic configurations. For all three compounds ΔE is negative meaning that the AFM state is the ground one reflecting the discussion in the last paragraph of the previous section. The values vary between -0.10 and -0.18 eV which are sizeable and suggest that the magnetic state should be feasible to stabilize in experiments like the ones of Jamer and collaborators.[21] Also in Table I we have included the atomic spin magnetic moments. The V^B and Al atoms have zero spin magnetic moments as expected since they

TABLE I: Calculated lattice parameters, total energy differences between non-magnetic and antiferromagnetic states, atom-resolved spin magnetic moments (in μ_B) and Néel temperatures for D0$_3$-type V$_3$Z (Z=Al, Ga, In) compounds. In parenthesis we show the LSDA results.

Compound	a(Å)	ΔE	$m^{\mathtt{A}}_{[\mathtt{V}]}$	$m^{\mathtt{B}}_{[\mathtt{V}]}$	$m^{\mathtt{C}}_{[\mathtt{V}]}$	$m^{\mathtt{D}}_{[\mathtt{Z}]}$	$T_{\mathrm{N}}^{\mathrm{RPA}}$ (K)
V$_3$Al	6.09	-0.12	-1.65 (-1.12)	0.00 (0.00)	1.65 (1.12)	0.00 (0.00)	988 (648)
V$_3$Ga	6.07	-0.10	-1.55 (-1.02)	0.00 (0.00)	1.55 (1.02)	0.00 (0.00)	858 (512)
V$_3$In	6.32	-0.18	-1.98 (-1.48)	0.00 (0.00)	1.98 (1.48)	0.00 (0.00)	1023 (704)

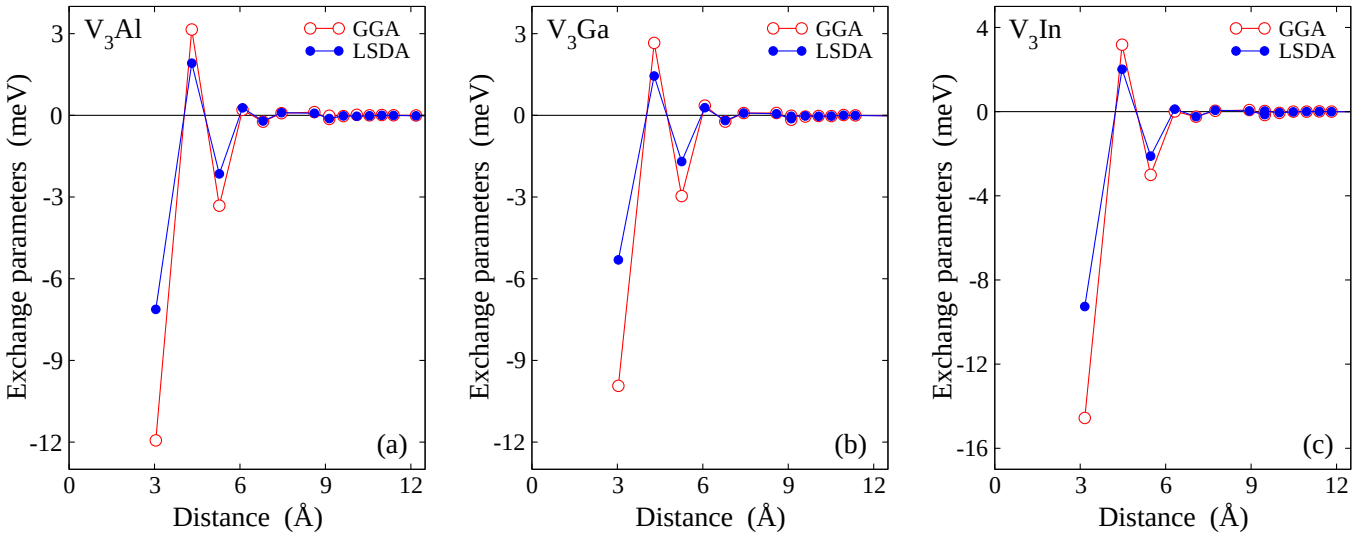

FIG. 4: (Color online) Interatomic exchange parameters (inter-sublattice V^A-V^C and intra-sublattice V^A-V^A) as a function of the distance for all three compounds under study using both GGA and LSDA functionals.

are at the midpoints between the V^A and V^C atoms. The latter one show considerable values of atomic spin magnetic moments, whose absolute values range from 1.55 μ_B in the case of V$_3$Ga to 1.98 μ_B for V$_3$In giving a first hint that exchange interaction should be strong leading to large values of the Néel temperature. Finally, if one looks at the structure presented in Fig. 1 neglecting the V^B and Al atoms, one can consider the structure of being build up by successive (111) plane made up of either pure V^A or V^C atoms. Thus two successive (111) planes have atoms of antiparallel spin magnetic moments and antiferromagnetism is of the so-called G-type shown in the lower panel of Fig. 1.

In Fig. 4 we present the calculated interatomic (intra-sublattice and inter-sublattice) exchange parameters involving the magnetic V atoms as a function of the distance. We can easily deduce from the figure that only interactions within the first three coordination shells are sizable. The first coordination shell concerns the inter-sublattice V^A-V^C exchange interactions (each V^A atom has V^B and Al atoms, which have zero spin magnetic moment, as nearest neighbors and six V^C atoms as next nearest neighbors) and it is the largest one providing the dominating contribution to the formation of the antiferromagnetic ground state and to the Néel temperature. The second coordination shell refers to the intra-sublattice V^A-V^A exchange interactions and it is of ferromagnetic character stabilizing further the antiferromagnetic state. Its value is considerably smaller than the absolute value of the exchange interaction between atoms in the 1st coordination shell due to the large distance between the V^A atoms in the lattice with respect to the V^A-V^C distance. Exchange interactions quickly decay with distance, which can be attributed to the existence of the gap in large part of the Brillouin zone shown in Fig. 8. This type of short-range behavior is typical of most half metallic magnets.[34,39]

RPA estimated Néel temperatures, $T_{\mathrm{N}}^{\mathrm{RPA}}$, within GGA are presented Table I. V$_3$Al shows a $T_{\mathrm{N}}^{\mathrm{RPA}}$ value of 988 K, V$_3$Ga of 858 K and V$_3$In of 1023 K. All these values are much larger than the room temperature ensuring that devices based on these compounds would be functional at room temperature. The experiments by Jamer and collaborators have provided a value of about 600 K for V$_3$Al,[21] which is considerably smaller than our value although it is still high compared to the room temperature. The discrepancy should be attributed to the character of the sample in Ref. 21. Our values concern bulk per-

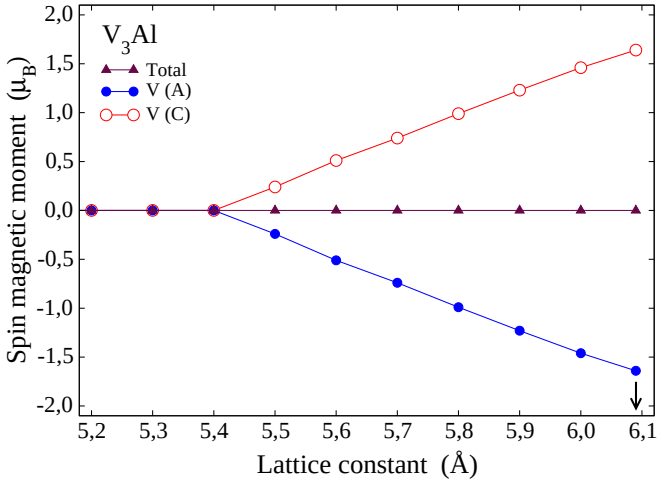

FIG. 5: (Color online) Atomic and total spin magnetic moments in the case of V_3Al upon compression starting from the equilibrium lattice constant marked by an arrow. Note that spin magnetic moment of the V atom at B site and Al atom at D site are zero due to symmetry reasons.

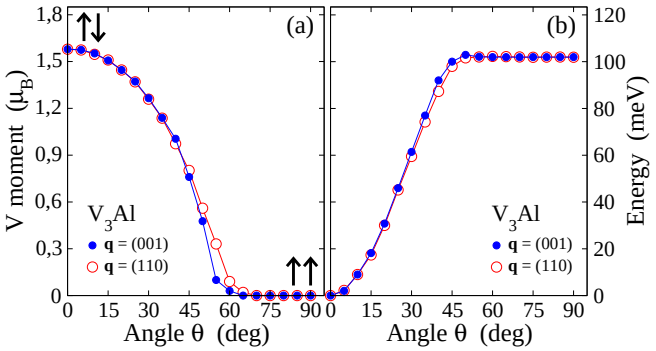

FIG. 6: (Color online) Behavior of the absolute values of the atomic spin magnetic moments of the V atoms at the A and C sites (left panel) and of the total energy (right panel) as a function of the polar angle θ (see Ref. 40) for two different values of the wave vector $\mathbf{q}$ (in units of $\frac{2\pi}{\alpha}$) in the case of the V_3Al compound. Notice that by varying θ between 0^o and 90^o for both wave vectors (001) and (110), the magnetic structure transforms continuously from the antiferromagnetic to the ferromagnetic configuration.

fect crystals while experiments have been performed on polycrystalline films prepared by arc melting. Even perfect thin films of a material present critical temperatures much smaller than bulk crystals of the same material and the discrepancy is much larger for polycrystalline films. Thus in reality the experimental value is consistent with our theoretical prediction.

Although the combination of GGA and RPA yields accurate critical temperature values in Heusler compounds,[34] it would be interesting to examine also the results of LSDA. As mentioned above LSDA overestimates the hybridization effect with respect to GGA resulting in considerable smaller values of the atomic spin magnetic moments in Table I. For example the absolute values of the V atomic spin magnetic moments in V_3Al decreases from 1.65 μ_B within GGA to 1.12 μ_B within LSDA a reduction of about 32 %. The smaller atomic spin magnetic moments also affect the exchange interactions in Fig. 4 which are smaller within LSDA resulting in smaller predicted values of the T_N^{RPA} in Table I. The discrepancy of the LSDA results with respect to the GGA ones provides a strong argument towards the character of the magnetism in the compounds under study. If magnetism was localized then the hybridization between the orbitals sitting at nearest sites would be negligible and both LSDA and GGA should give similar results. When magnetism is of itinerant character, the hybridization between orbitals of nearest sites is important and LSDA and GGA would give a sizeable discrepancy between the computed magnetic properties. This is the case and thus we can conclude that in V_3Al, V_3Ga and V_3In compounds the antiferromagnetism is of itinerant character.

Another characteristic supporting this conclusion is the behavior of the atomic spin magnetic moments under compression. If their values persist then magnetism is of localized character, while if it goes fast to zero magnetism is of itinerant character since compression fast reduces and eventually kills the hybridization effect. This has been clearly demonstrated in the case of Cr_3Se where both kind of magnetic behaviors coexist.[18] We have plotted the behavior of the GGA atomic spin magnetic moments under compression in Fig. 5. As we compress the lattice and the lattice constant is reduced, the absolute values of the spin magnetic moments of both V^A and V^C atoms present a linear reduction vanishing at about 5.4 Å and the compound remains a perfect antiferromagnet under this compression. This behavior is compatible with the itinerant character of magnetism discussed in the above paragraph.

Our final step in the investigation of the magnetic properties of the compounds under study is the stability of the AFM state with respect to ferromagnetic ordering. In Fig. 6 we have plotted for V_3Al the variation of the absolute values of the atomic spin magnetic moments of the V atoms at the A and C sites (left panel) as a function of the polar angle θ. On the right panel we plotted the behavior of the total energy as a function of the polar angle. We took into account two different values of the wave vector $\mathbf{q}$ (in units of $\frac{2\pi}{\alpha}$): the (001) and (110). The reason is that for these two values the magnetic structure transforms continuously from the antiferromagnetic to the ferromagnetic configuration as the θ angle changes from 0^o to 90^o. The curves for both $\mathbf{q}$ values are similar leading to the same conclusions. As the angle θ increases and the spin magnetic moments rotate to the ferromagnetic configuration the absolute values of the spin moments decrease and simultaneously the total energy increases reaching a maximum at about 45^o. The minimum of the total energy corresponds to an angle of

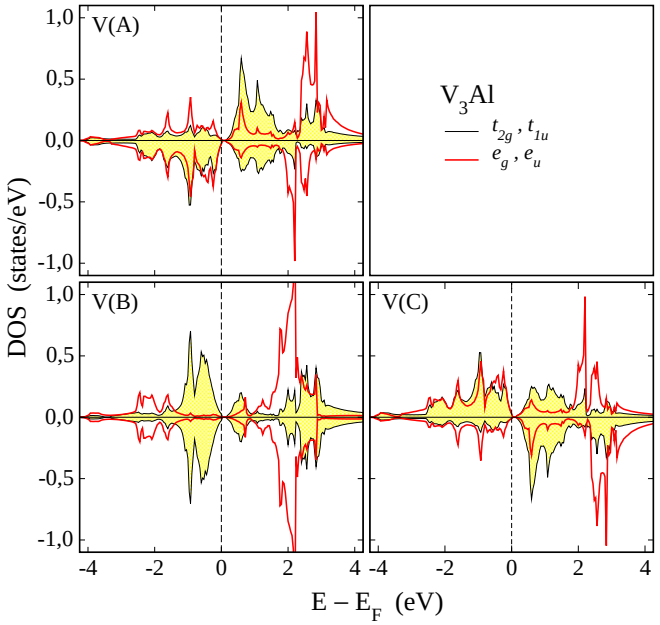

FIG. 7: (Color online) DOS for the V atoms in V_3Al projected on the double degenerate e_g and e_u, and the triple degenerate t_{2g} and t_{1u} d-states. Note that we cannot distinguish between the g-type states obeying both the octahedral and tetrahedral symmetry and the u-type states obeying exclusively the octahedral symmetry.

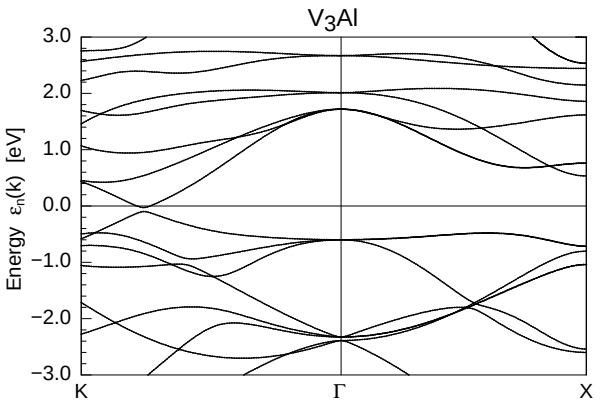

FIG. 8: Band structure along two high-symmetry axis. There is a direct gap at about one fourth the distance between the K and the Γ high symmetry points. For the character of the bands see Fig. 9 and discussion in the text

0^o and thus to the antiferromagnetic coupling of the spin magnetic moments of the V^A and V^C atoms.

C. Origin of the gapless behavior

In the last part of the discussion of the results, we will concentrate on the origin of the gapless behavior using arguments similar to the one used for the full and the inverse Heusler compounds.[10,11] Again we will use V_3Al as the prototype but results are similar also for the V_3Ga and V_3In compounds. First as for the full Heuslers, we can have two type of d-orbitals. The ones concentrated exclusively at the V^A and V^C sites. These atoms create a simple cubic structure, if we neglect the V^B and Al atoms, and thus due to symmetry reasons d-hybrids of u type obeying the octahedral symmetry and being localized exclusively at the V^A and V^C sites are allowed. These can be distinguished between the double-degenerate e_u and the triple-degenerate t_{1u} states. Except the states of the u character we can also have states of g character which obey both the octahedral and tetrahedral symmetry and are delocalized to all sites. They also break down to the double-degenerate e_g and the triple-degenerate t_{2g} states. In the tetrahedral symmetry the e_g states are lower in energy than the t_{2g} states, while in the octahedral symmetry it is vice versa and the t_{1u} states are below the e_u states. In Fig. 7 we have projected the atom-resolved DOS on the different g and u states. Note that we cannot distinguish the $e_u(t_{1u})$ from the $e_g(t_{2g})$ states. The V^A and V^C atoms posses states of both character from both sides of the gap. In the case of V^B atoms, the states deeper in energy are of e_g character while below the Fermi level states are exclusively of t_{2g} character (note that the u states are not allowed at the V^B site). Above the Fermi level we can find states of both characters.

To make a step further in our understanding of the origin of the gapless semiconducting behavior we have plotted in Fig. 8 the band structure along the K-Γ and Γ-X lines. Note that the band structure is identical for both spin-directions. Examining the band structure along several directions (not shown here) reveals that there is a direct gap of vanishing width located at about the $\frac{1}{4}$ the K-Γ distance. Just below the Fermi level there is a triple-degenerate (at the Γ-point) band. Deeper in energy at about -2.5 eV below the Fermi level, at the Γ-point there are very close in energy a triple and a double degenerate bands. Lower in energy (not shown here) is a single band. Above the Fermi level we have a triple-degenerate (at the Γ-point) band followed by two double-degenerate (at the Γ-point) bands. The character of the bands at the Γ-point is primordial for our understanding of the origin of the gapless behavior since it reveals also the character of the bands at the real space and it has been extensively used in the case of Heusler compounds.[10,11]

To reveal the character of each band we have performed an analysis based on the fat band scheme which we have also employed in the case of the Cr_3Se compounds in Ref. 18. We do not show all band structure here but we resume our results in Fig. 9 where for one spin-direction we present the character of the bands. First, we have to note that V_3Al has 18 valence electrons per formula unit (it coincides with the per unit cell value) and thus per spin we should have 9 occupied states. As for the minority-band structures of full and inverse Heusler compounds which show the semiconducting behavior (see

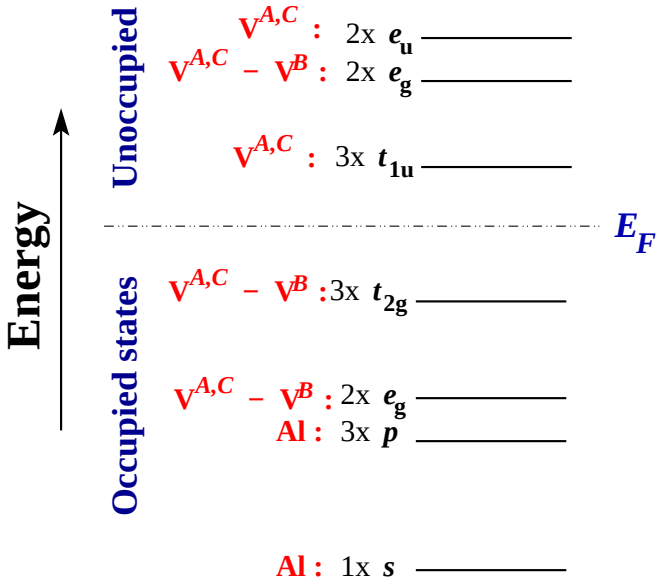

FIG. 9: (Color online) Schematic representation of the character of the bands at the Γ-point which corresponds to the character of the orbitals in real space, based on the atom and orbital resolved bands using the fat band scheme (not shown here). Notice that the low-lying Al p bands accommodate also a large portion of V's d charge and thus have a strong admixture of the $V^{A,C}$ triple-degenerate t_{2g} states.

Refs. 10 and 11), the single band low in energy stems from the Al valence s-state. At about -2.5 eV there are very close in energy at the Γ point the triple-band stemming from the Al p-states accommodating also d charge from the V atoms, and the double-band stemming from the e_g states which are spread over all V atoms. Just below the Fermi level the triple degenerate valence band has a t_{2g} character and the corresponding orbitals are located at all V sites; these bands have also a strong Al p-admixture since the t_{2g} states when expressed around the Al site have a p character. The first bands above the Fermi level are the triple-degenerate t_{1u} bands located mainly at the V^A and V^C sites followed by the e_g and e_u bands. Thus the Fermi level is located between the occupied t_{2g} and the empty t_{1u} states. This resembles the hybridization scheme in the case of the Sc- and Ti-based inverse Heusler compounds in Ref. 11. The gap in the latter case is small since it does not result from a bonding-antibonding hybrid formation, and in the case of V_3Al its width is vanishing since both X and Y atoms in the X_2YZ formula of the inverse Heuslers are identical and the energy levels in the upper panel of figure 3 in Ref. 11 are much closer closing the gap separating the t_{2g} and the t_{1u} states. This explains the gapless character of V_3Al.

IV. CONCLUSIONS

Heusler compounds are widely studied due to their variety of magnetic properties which they present. Especially for spintronics and magnetoelectronics, properties like half-metallicity or spin-gapless semiconducting behavior are crucial to enhance the functionalities of realistic devices. This interest has been triggered both by the advances in computational materials science, which permit the accurate modelling of several complex materials, and the advances in the synthesis and growth of materials which enables the growth of materials in new metastable structures. To this aspect the prediction of antiferromagnetic gapless behavior in the case of V_3Al adopting the metastable Heusler structure (Ref. 14) and its successful growth (Ref. 21) pave the way for the incorporation of this materials in realistic devices.

We have provided an extensive study on the electronic and magnetic properties of V_3Al compound as well as its isovalent V_3Ga and V_3In compounds using state-of-the-art electronic structure calculations. All compounds prefer the gapless G-type antiferromagnetic structure. The large absolute values of the spin magnetic moments of the V atoms having antiparallel spin moments lead to a strong short-range exchange interaction and consequently to high value of the Néel temperature which approaches or even exceeds 1000 K making them operational at room temperature. The G-type antiferromagnetism is stable with respect to the ferromagnetic configuration and it proves to be of strongly itinerant character. Finally, we discussed the origin of the gapless behavior. We have shown that the character of the bands is similar to the inverse Heusler compounds studied in Ref. 11 but the presence of three V atoms at the unit cell closes the gap leading to the gapless character.

We expect our study on V_3Al, V_3Ga and V_3In compounds to enhance further the interest on them. Based on our results and the experiments in Ref. 21, further experiments are needed to establish a grown mechanism optimizing the magnetic and structural properties of these compounds in the metastable Heusler structure leading to their eventual incorporation in devices.

* Electronic address: galanakis@upatras.gr
† Electronic address: e.sasioglu@gmail.com

[1] F. Heusler, Verh. Dtsch. Phys. Ges. **12**, 219 (1903).
[2] C. Felser, G. H. Fecher, and B. Balke, Angew. Chem. Int. Ed. **46**, 668 (2007).
[3] T. Graf, C. Felser, and S. S. P. Parkin , Progress in Solid State Chemistry **39**, 1 (2011).
[4] M. Gillessen and R. Dronskowski, J. Comput. Chem. **30**, 1290 (2009).
[5] M. Gillessen and R. Dronskowski, J. Comput. Chem. **31**, 612 (2010).
[6] I. Žutić, J. Fabian, and S. Das Sarma, Rev. Mod. Phys. 76 (2004) 323.
[7] M. Bowen, A. Barthélèmy, M. Bibes, E. Jacquet, J. P.

Contour, A. Fert, D. Wortmann, and S. Blügel, J. Phys.: Condens. Matter **17**, L407 (2005).

[8] P.J. Webster and K.R.A. Ziebeck. In: *Alloys and Compounds of d-Elements with Main Group Elements. Part 2.*, Landolt-Börnstein, New Series, Group III, vol 19c, ed by H.R.J. Wijn, (Springer, Berlin 1988) pp 75–184.

[9] K.R.A. Ziebeck and K.-U. Neumann. In: *Magnetic Properties of Metals*, Landolt-Börnstein, New Series, Group III, vol 32/c, ed by H.R.J. Wijn, (Springer, Berlin 2001) pp 64–414.

[10] I. Galanakis, P. H. Dederichs, and N. Papanikolaou, Phys. Rev. B **66**, 174429 (2002).

[11] S. Skaftouros, K. Özdoğan, E. Şaşıoğlu, and I. Galanakis, Phys. Rev. B **87**, 024420 (2013).

[12] A. Hirohata and K. Takanashi, J. Phys. D: Appl. Phys. **47**, 193001 (2014).

[13] X. L. Wang, Phys. Rev. Lett. **100**, 156404 (2008).

[14] S. Skaftouros, K. Özdoğan, E. Şaşıoğlu, and I. Galanakis, Appl. Phys. Lett. **102**, 022402 (2013).

[15] A. Jakobsson, P. Mavropoulos, E. Şaşıoğlu, S. Blügel, M. Ležaić, B. Sanyal, and I. Galanakis, Phys. Rev. B **91**, 174439 (2015).

[16] S. Ouardi, G. H. Fecher, C. Felser, and J. Kübler, Phys. Rev. Lett. **110**, 100401 (2013).

[17] Joo Yull Rhee and B. N. Harmon Phys. Rev. B **70**, 094411 (2004).

[18] I. Galanakis, K. Özdoğan, and E. Şaşıoğlu, Phys. Rev. B **86**, 134427 (2012).

[19] G. Y. Gao and K.-L. Yao, Appl. Phys. Lett. **103**, 232409

[20] Isaak M. Tsidilkovski, in *Electron Spectrum of Gapless Semiconductors*, edited by Klaus von Klitzing, Springer Series in Solid-State Sciences Vol. 116 (Springer, New York, 1996).

[21] M. E. Jamer, B. A. Assaf, G. E. Sterbinsky, D. Arena, L. H. Lewis, A. A. Saúl, G. Radtke, and D. Heiman, Phys. Rev. B **91**, 094409 (2015).

[22] L. R. Testardi, T. Wakiyama, and W. A. Royer, J. Appl. Phys. **48**, 2055, (1977).

[23] S. Ohshima, H. Ishida, T. Wakiyama, and K. Okuyama, Jpn. J. Appl. Phys. **28**, 1362 (1989).

[24] K. Koepernik and H. Eschrig, Phys. Rev. B **59**, 1743 (1999).

[25] K. Kopernik, Full Potential Local Orbital Minimum Basis Bandstructure Scheme Users Manual (http://www.fplo.de/download/ doc.pdf).

[26] J. P. Perdew, K. Burke, and M. Ernzerhof, Phys. Rev. Lett. **77**, 3865 (1996).

[27] J. P. Perdew and Y. Wang, Phys. Rev. B **45**, 13244 (1992).

[28] H. J. Monkhorst and J. D. Pack, Phys. Rev. B **13**, 5188 (1976).

[29] A. R. Williams, J. Kübler, and C. D. Gelatt, Phys. Rev. B **19**, 6094(1979).

[30] N. M. Rosengaard and B. Johansson, Phys. Rev. B **55** 14975 (1997).

[31] S. V. Halilov, H. Eschrig, A. Ya. Perlov, and P. M. Oppeneer, Phys. Rev. B **58** 293 (1998).

[32] L. M. Sandratskii and P. Bruno, Phys. Rev. B **67**, 214402 (2003).

[33] E. Şaşıoğlu, L. M. Sandratskii, and P. Bruno, Phys. Rev. B **70**, 024427 (2004).

[34] E. Şaşıoğlu, L. M. Sandratskii, P. Bruno, and I. Galanakis, Phys. Rev. B **72**, 184415 (2005).

[35] S. V. Tyablikov, *Methods of Quantum Theory of Magnetism* (Plenum Press, New York, 1967)

[36] H. B. Callen, Phys. Rev. **130** 890 (1963)

[37] M. Pajda, J. Kudrnovsky, I. Turek, V. Drchal, and P. Bruno, Phys. Rev. B **64**, 174402 (2001).

[38] G. Bouzerar, J. Kudrnovský, L. Bergqvist, and P. Bruno, Phys. Rev. B **68**, 081203 (2003).

[39] J. Rusz, L. Bergqvist, J. Kudrnovský, and I. Turek Phys. Rev. B **73**, 214412 (2006).

[40] E. Şaşıoğlu, L. M. Sandratskii, and P. Bruno Phys. Rev. B **77**, 064417 (2008).